THE JOURNAL OF PHYSICAL CHEMISTRY C

ARTICLE

pubs.acs.org/JPCC

Adsorption and Diffusion of Fructose in Zeolite HZSM-5: Selection of Models and Methods for Computational Studies

Lei Cheng,[†] Larry A. Curtiss,[*,†,‡] Rajeev Surendran Assary,[†,§] Jeffrey Greeley,[‡] Torsten Kerber,[⊥] and Joachim Sauer[⊥]

[†]Materials Science Division, Argonne National Laboratory, Argonne, Illinois 60439, United States

[‡]Center for Nanoscale Materials, Argonne National Laboratory, Argonne, Illinois 60439, United States

[§]Chemical & Biological Engineering, Northwestern University, Evanston, Illinois 60208, United States

[⊥]Institut für Chemie, Humboldt-Universität zu Berlin, D-10099 Berlin, Germany

ABSTRACT: The adsorption and protonation of fructose in HZSM-5 have been studied for the assessment of models for accurate reaction energy calculations and the evaluation of molecular diffusivity. The adsorption and protonation were calculated using 2T, 5T, and 46T clusters as well as a periodic model. The results indicate that the reaction thermodynamics cannot be predicted correctly using small cluster models, such as 2T or 5T, because these small cluster models fail to represent the electrostatic effect of a zeolite cage, which provides additional stabilization to the ion pair formed upon the protonation of fructose. Structural parameters optimized using the 46T cluster model agree well with those of the full periodic model; however, the calculated reaction energies are in significant error due to the poor account of dispersion effects by density functional theory. The dispersion effects contribute −30.5 kcal/mol to the binding energy of fructose in the zeolite pore based on periodic model calculations that include dispersion interactions. The protonation of the fructose ternary carbon hydroxyl group was calculated to be exothermic by 5.5 kcal/mol with a reaction barrier of 2.9 kcal/mol using the periodic model with dispersion effects. Our results suggest that the internal diffusion of fructose in HZSM-5 is very likely to be energetically limited and only occurs at high temperature due to the large size of the molecule.

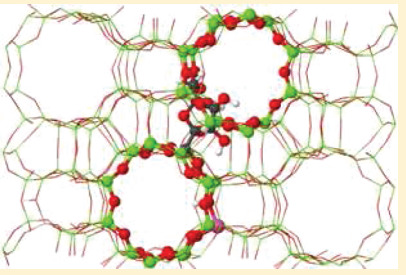

1. INTRODUCTION

Biomass has the potential to serve as a renewable energy source and to produce industrially important chemicals. However, achieving controlled, energy-efficient conversion of cellulose to potentially useful chemicals poses a great challenge in catalysis science. Conversion of biomass to fuels and value-added chemicals is a very complex process.[1] It involves, first, the hydrolysis of cellulose to carbohydrates, followed by targeted dehydration, hydrogenolysis, dehydrogenation, hydrogenation, oxidation, etc. In a recent computational study[2] of the conversion of glucose to 5-hydroxy methyl furfural (HMF), levulinic acid, and formic acid in a homogeneous environment, the thermochemical data were computed for the isomerization of glucose to more active fructose species and for the subsequent three targeted dehydration steps that complete the conversion to HMF. However, no computational studies of fructose activation in solid acid catalysts have been reported. Experimentally, mineral acids in solution and acid sites on solid Brønsted catalysts are commonly used to dehydrate hexoses.[3,4] Several research groups have used zeolites or acid ion-exchange resins to prepare HMF from fructose dehydration.[5−9] Zeolite HZSM-5 is a very versatile catalyst and can be used as a solid acid for a range of reactions, such as alcohol dehydration, hydrocarbon isomerization, and alkylation. It has also been used previously in catalytic fast pyrolysis for biofuel production.[10,11]

Computational studies can help understand reaction mechanisms and predict the thermodynamics, kinetics, and pore selectivities of the reactions catalyzed by zeolites, such as those involving fructose. Applying appropriate theoretical treatments to these studies of zeolites is crucial. Density functional theory (DFT) is computationally cost-efficient and has been routinely used in the computational catalysis community. However, the method suffers from the disadvantage of not accounting for long-range dispersion interactions properly, and this limits its application in many reactions catalyzed by zeolites. Tuma and Sauer applied a hybrid MP2:DFT scheme[12] to add the MP2 corrections to reaction energies in the full periodic limit. The scheme can accurately calculate bond rearrangement and dispersion interactions at the same time and yields reaction barriers comparable with the experimental data.[13,14] However, such an approach requires many expensive MP2 calculations of cluster models for the extrapolation of the final reaction energy to the periodic limit. Alternatively, a computationally less expensive scheme with an added damped C_6 dispersion term parametrized by Grimme[15] to the full periodic PBE energies[16] (PBE+D) was found to yield reaction energies comparable to those predicted by the hybrid method for the methylation of alkenes[13] and the alkylation of benzene in HZSM-5.[17] In comparison to the DFT calculations, the PBE+D reaction potential energy profile was shifted downward significantly

Received: June 30, 2011
Revised: September 8, 2011
Published: September 14, 2011

due to the dispersion interaction between the reactant molecule and the zeolite lattice.

In this work, we have studied HZSM-5 as a solid Brønsted acid catalyst for fructose decomposition. The goals of this work were two-fold. First, we sought to determine the computational requirements for accurate calculations of a system, such as fructose in an HZSM-5 pore, including the effects of dispersion, which have been found to be important for other zeolite reactions, and the size of the cluster model required to converge to the periodic limit. The second goal was to determine with accurate calculations the adsorption energies and the barrier for protonation of fructose in the HZSM-5 zeolite, together with the diffusion rate of the molecule. In the following section (2), we describe the methods used in this study. In section 3, we report the reaction energies of β-D-fructose adsorption and protonation (the first two steps of acid catalysis) with small 2T and 5T clusters that only model the acidic site of zeolite HZSM-5. We then extend the calculations to a 46T cage structure that describes the active site as well as the zeolite framework effect. The 46T model has previously been successfully used in the literature for zeolite studies.[18−20] The results calculated using the cluster models were then compared with the benchmark results calculated using full periodic DFT+D with cluster model MP2/CBS (complete basis set) corrections (see section 2 for details). In addition, to predict whether the interior mass transfer of fructose in HZSM-5 is limited, we also calculated and compared the fructose adsorption energies in the zeolite straight channel and the channel intersection using a periodic model. Conclusions are reported in section 4.

2. COMPUTATIONAL MODEL AND METHODS

The 2T and 5T clusters representing the reaction center of the zeolite were truncated from the full siliceous crystallographic ZSM-5 structure[21] and terminated with H atoms. One Si atom in the cluster was replaced by an Al atom, and a proton was added to balance the charge and create an acidic site. All atoms were allowed to relax for the optimizations using the two cluster models. Structure optimizations of fructose adsorption on the 2T cluster with the 6-31G* basis set were performed using the following functionals: B3LYP,[22] PBE,[23] PW91,[24] and M05.[25] Two other basis sets, 6-31G(2df,p) and LANL2DZP, were also used with the B3LYP functional optimization. A PW91 optimization was done with a plane-wave (PW) basis set. In addition, a damped C_6 term parametrized by Grimme[15] was added to the PW91/PW potential (PW91+D) for structure optimizations.[16] The s_6 scale factor of 0.75, which was originally determined for the PBE functional in Grimme's work, has been used. At the B3LYP/6-31G* optimized geometry, the B3LYP/6-31+G* energy calculation was carried out; at the B3LYP/6-31G(2df,p) optimized geometry, an energy calculation with the G3MP2Large basis set was performed; at PW91+D/PW optimized geometry, the MP2 energies with the cc-pVTZ and cc-pQTZ basis sets were calculated and extrapolated to the CBS limit (MP2/CBS), as in previous work.[12] Optimizations of the fructose adsorption on a 5T cluster were performed at the B3LYP/6-31G*, B3LYP/6-31G(2df,p), PW91/6-31G*, PW91/6-31G(2df,p), and PW91/PW levels. The calculations of the 46T clusters and the periodic models were carried out using PW91/PW. The same 46T model has previously been used to illustrate the shape selectivity of different zeolites[26] as well as to calculate the relative activation energies of different reactant species.[27] In the 46T model, the active site was created at the T_1 position.[28] All terminating hydrogen atoms in the 46T cluster were fixed, while the rest were allowed to relax during optimization. The full periodic unit cell model also has the active site located at the T_1 position. All 313 atoms, including the reactant molecule and the zeolite, were allowed to relax while the lattice parameters of a full siliceous ZSM-5[21,29] were used for the unit cell and kept constant during optimizations since the Al/Si ratio in the model is very low (1:95). Furthermore, at each periodic PW91+D structure, an OH-terminated 5T cluster was truncated along with the adsorbed molecule (5T//periodic). The MP2/CBS adsorption energies of these 5T//periodic clusters were then calculated using the same extrapolation scheme mentioned above. The difference between the MP2/CBS and PW91+D adsorption energies of a 5T// periodic cluster is then used to add a higher-order correction to the calculated periodic PW91+D reaction energy.

Our calculations in this work were carried out using the Gaussian 09,[30] VASP,[31] and NWChem[32] codes. The cutoff energy of the PW basis set in the VASP calculations was chosen to be 400 eV. The Γ-point and the 2 × 2 × 1 *k*-points mesh, respectively, were used to sample the Brillouin zones in the cluster and periodic calculations.

Adsorption energies were calculated using the equation

$$E_{ads} = E_{fruc+HZSM\text{-}5} - (E_{fruc} + E_{HZSM\text{-}5}) \quad (1)$$

where $E_{fruc+HZSM\text{-}5}$, E_{fruc}, and $E_{HZSM\text{-}5}$ are total electronic energies of the fructose−zeolite complex, the fructose molecule, and the zeolite model, respectively, at the same theory and basis set level. Water molecules in zeolite cages are expected to compete with the reactant molecules for protons or to act as proton transporters. However, we did not include any water molecules in our calculations because the primary goal of this study is to benchmark computational models and methods, and this goal will not be affected by the inclusion of water molecules.

3. RESULTS AND DISCUSSION

3.1. Fructose Adsorption and Protonation on 2T and 5T Cluster Models. The initial structures of fructose adsorption on 2T and 5T clusters were set up to have a similar bonding structure as the most stable adsorption geometry found for fructose adsorption in an HZSM-5 zigzag pore using a periodic model. In the optimized fructose adsorption structure on 2T, shown in Figure 1a, the molecule is coordinated to the zeolite acidic site through the oxygen atom of the hydroxyl group of the ternary carbon atom (C_2). In the optimized fructose adsorption structure on the 5T cluster, shown in Figure 1b, in addition to the similar bonding as in the 2T cluster, the hydroxyl group of the C_1 atom also forms a hydrogen bond with an oxygen atom of the cluster (O_s). The adsorption energies calculated using both of these models with basis set superposition error (BSSE) corrections are reported in Table 1. The BSSE corrections reduce the basis set dependence, as expected. We, therefore, discuss the BSSE-corrected values only. Note that there is no BSSE if plane waves are used as the basis set, and for example, the BSSE-corrected PW91/6-31G* result agrees nicely with the PW91/PW result for both the 2T and the 5T models.

The B3LYP binding energies of fructose on the 2T cluster reported in Table 1 are all in the range of −9 to −10 kcal/mol, with the exception of the value calculated using the effective core potential basis set LANL2DZ, which predicts much stronger binding (more negative binding energy). The B3LYP binding energies of fructose on 5T are −16 to −17 kcal/mol. With the largest basis set, G3MP2L,[33] the B3LYP result is −9.1 kcal/mol

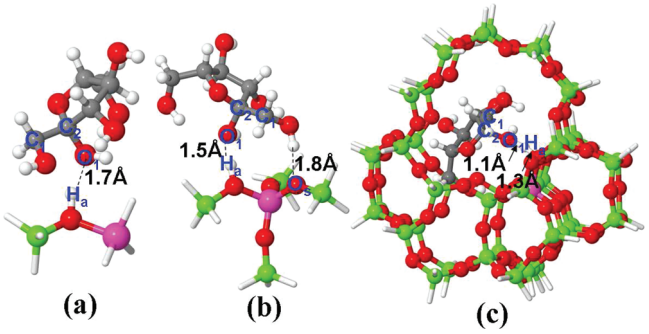

Figure 1. Optimized structures of fructose adsorption on the (a) 2T, (b) 5T, and (c) 46T HZSM-5 models (gray, C; white, H; red, O; pink, Al; green, Si).

Table 1. Energies of Adsorption (kcal/mol) of Fructose on 2T and 5T Zeolite Models[a]

method	2T model	5T model
B3LYP/LANL2DZP	−19.6 (−22.4)	
B3LYP/6-31G*	−9.7 (−14.3)	−17.2 (−24.4)
B3LYP/6-31+G*//B3LYP/6-31G*	−8.6 (−10.8)	
B3LYP/6-31G(2df,p)	−9.5 (−14.5)	−15.9 (−22.8)
B3LYP/G3MP2L//B3LYP/6-31G (2df,p)	−9.1 (−10.1)	
M05/6-31G*	−11.4 (−15.9)	
PBE/6-31G*	−11.5 (−16.6)	
PW91/6-31G*	−12.0 (−17.3)	−21.0 (−29.3)
PW91/plane wave	−12.0[b]	−21.0[b]
PW91+D/plane wave	−15.1[b]	−27.8[b]
MP2/CBS// PW91+D/plane wave	−13.9	
MP2/6-31G*	−16.6	
CCSD(T)/6-31G*//MP2/6-31G*	−16.2	

[a] The energies are corrected for the basis set superposition error (BSSE). Uncorrected values are shown in parentheses. [b] The plane-wave results are BSSE-free.

for the 2T model. This value lacks contributions from dispersion. The M05 and the PW91 functionals take into account missing dispersion contributions, thus yielding 1.7 and 2.3 kcal/mol, stronger binding, respectively, than the B3LYP functional. Inclusion of long-range dispersion by adding the semiempirical $1/r^6$ term to the PW91 functional (PW91+D/PW) increases the binding energy by 3.1 kcal/mol for the 2T model and by as much as 6.8 kcal/mol for the larger 5T model. The MP2/CBS method is the highest level of this series of calculations. It predicts weaker binding than PW91+D, which may be due to both proper self-interaction correction and improved descriptions of dispersion. To estimate the role of higher-order correlation effects, CCSD(T) and MP2 calculations have been performed with the 6-31G* basis set. A small reduction of the binding energy (by 0.4 kcal/mol) is predicted with CCSD(T). Additionally, the structure optimized with the MP2/6-31G* method is very similar to that of the DFT; for example, the O_1-H_a bond distance was calculated to be 1.7 Å with the MP 2/6-31G*, B3LYP/6-31G*, and PW 91/6-31G* optimizations, indicating the reliability of the DFT methods.

Upon fructose adsorption, the reaction catalyzed by the acidic site proceeds with protonation of the reactant molecule. The C_2 hydroxyl group has the largest proton affinity among all hydroxyl groups and thus is most likely to be protonated first during reaction.[2] Previously, cluster models have been used by many groups to study the proton transfer from a zeolite acidic site to water,[34−36] and those studies successfully predicted results consistent with experimental observations. In this work, we attempted to calculate an ion pair structure with the proton of the zeolite cluster transferred to the adsorbed fructose molecule. Previous theoretical work predicts that a molecule can be protonated by an H-zeolite when its proton affinity is higher than 204 kcal/mol.[37,38] The proton affinity of the tertiary hydroxyl group of the fructose was calculated to be 209.4 kcal/mol at the G4 level,[39] suggesting that protonation of the molecule should occur. However, we were not able to find a stable ion pair structure with either the 2T or the 5T cluster. This is probably because the electrostatic effect of the zeolite framework, which is known to stabilize ion pairs, is not well represented by small clusters, such as 2T and 5T. Unlike water, the fructose molecule is rather large, so the additional electrostatic stabilization effect may also be very important. Thus, small cluster models fail to represent the reactivity of the zeolite acidic site, and calculations using more advanced models are required.

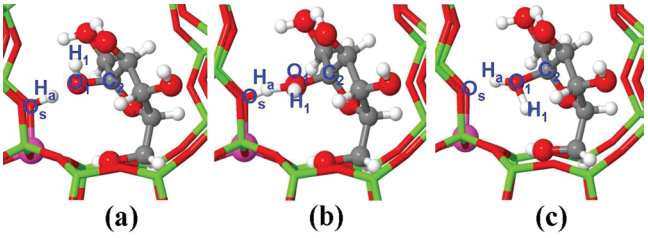

Figure 2. Structures of a fructose (a) adsorption and (c) protonation in an HZSM-5 channel intersection optimized using the periodic PW91+D method. The proton-transfer transition-state structure is shown in (b).

3.2. Fructose Adsorption and Protonation on 46T and Periodic Models. Inside a ZSM-5 lattice, the intersection of the straight and sinusoidal channels has the largest "opening" and is where large reactant molecules are expected to adsorb most strongly. The calculated structure of adsorbed fructose at the channel intersection using a 46T cluster is shown in Figure 1c. The structure with the proton transferred from the zeolite to the fructose molecule in the 46T cluster was found to be a stable structure (not shown). The calculated structures for fructose in a periodic model of HZSM-5 are shown in Figure 2. The optimized adsorbed structure is shown in Figure 2a. The structure of the protonated fructose in the periodic model is shown in Figure 2c. Frequency calculations confirmed that these structures are local minima.

The adsorption and protonation reaction energies calculated for these two models are plotted in Figure 3. The result for the periodic limit indicates that, even at cluster size 46T, the adsorption energies (46T, PW91+D) differ by 8.6 kcal/mol from the periodic results (periodic, PW91+D). This is because the long-range dispersion interaction converges slowly to the periodic limit with the increasing cluster size, as shown previously.[12] The PW91 adsorption energy of the 46T (46T, PW91) cluster without dispersion energy differs from the periodic result (periodic, PW91) by a smaller, but still significant, amount, 4 kcal/mol. Despite the energy differences, the key structural parameters, such as bond lengths and bond angles, optimized using the two models (46T and periodic) are very similar. For example, the distance between the zeolite acidic site and the oxygen of the fructose hydroxyl group (H_a-O_1) was calculated to be 1.3 Å in both models (Figures 1c and 2a).

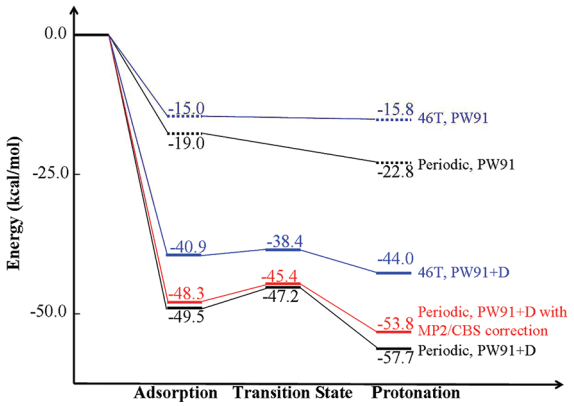

Figure 3. Potential energy profile of fructose adsorption and protonation in HZSM-5 calculated using the 46T and periodic models. All energies are calculated at the PW91+D geometries.

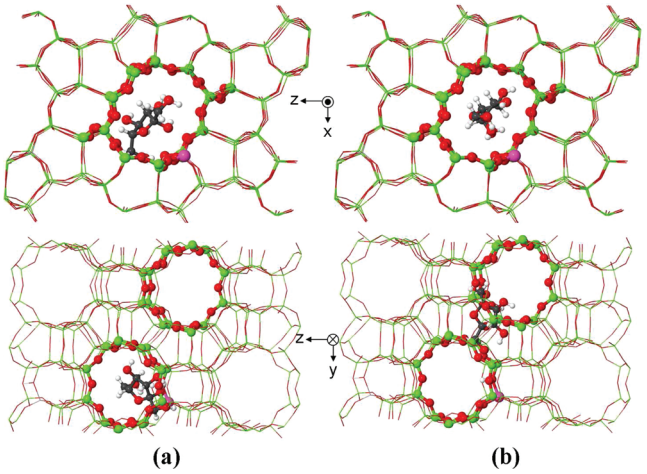

Figure 4. Illustrations from two perspectives (top and bottom) of fructose positions in the most stable adsorption configuration (a) at a sinusoidal and straight channel intersection and (b) in a straight channel position where two channels do not intersect. A (1 × 1 × 2) cell is shown in each figure, and the atoms at the intersections of a straight and a zigzag channel along with fructose are shown in ball and stick.

The dispersion interaction contributes significantly to the adsorption energies of the periodic model. The dispersion contributes −30.5 kcal/mol to the total adsorption energy of −49.5 kcal/mol (periodic, PW91+D). The −30.5 kcal/mol dispersion energy originates from nonbonding interactions between the fructose molecule and the zeolite framework and should be approximately the minimum binding of a fructose molecule adsorbed at such a position in the zeolite cage, regardless of the acidic site positions; if the fructose molecule binds at a nearby zeolite acidic site, the adsorption should be exothermic by at least −30.5 kcal/mol. An even larger dispersion contribution of −34.9 kcal/mol is found for the protonation reaction energy. The MP2/CBS adsorption energy calculation of the fructose adsorption 5T//periodic cluster adds a correction of 1.2 kcal/mol to the PW91+D adsorption energy, and the final adsorption energy of the full periodic system was evaluated to be −48.3 kcal/mol (shown in Figure 3). The MP2/CBS correction for the protonated structure is 3.9 kcal/mol, so the final reaction energy for the protonated structure is −53.8 kcal/mol. The MP2/CBS corrections are larger for the protonated structure (3.9 kcal/mol) than for the neutral adsorption structure (1.2 kcal/mol), reflecting the overstabilization of polar structures by GGA functionals.[12,13,40] Compared to the large effect of including dispersion, this effect is small, suggesting that the PW91+D reaction energies are accurate to within a few kcal/mol.

The transition state of the proton transfer was located, and the structure is shown in Figure 2b. The proton transfer is a rather interesting process: The H_1 atom of the fructose that initially forms an internal hydrogen bond with another hydroxyl group from the molecule (Figure 2a) first rotates "down" to a position, as in the transition structure shown in Figure 2b. The H_1 then rotates further to form a hydrogen bond with the O_2 atom, and at the same time, the H_a transfers from the zeolite to the fructose molecule. Because the H_a atom is partially bonded to the O_1 atom (1.3 Å) in the initial structure, once the system passes the H_1 rotation barrier, the proton transfer itself is energetically downhill. Thus, the imaginary frequency of the transition state corresponds to a rotational mode of H_1. The PW91+D reaction energy of this transition state is −47.2 and −45.4 kcal/mol with the MP2/CBS correction. This corresponds to an intrinsic barrier of only 2.9 kcal/mol, meaning that the proton transfer is a relatively easy step and should not limit the reaction rate.

3.3. Molecular Diffusion. Internal diffusion of reactant molecules is of great concern when microporous zeolites, especially medium-sized zeolites, such as ZSM-5, are used as catalysts for large molecule conversions. It was previously reported in the literature that fructose does not adsorb on ZMS-5 at 25 °C in water solution.[41] For a fructose molecule to reach the interior of the zeolite bulk instead of reacting solely on the external crystal surface, the molecule has to be able to diffuse through the elliptical-shaped 10-membered rings that comprise the "straight channel" of the ZSM-5. Calculating the diffusion barrier is very complicated. For example, the conformation of the fructose molecule might change during the migration, and multiple steps might be involved in the process. However, we can get a rough estimate of whether the diffusion is limited by calculating the fructose adsorption structure in the straight pore where the channel does not intersect with others and the opening is the narrowest. We have calculated several adsorption configurations of fructose in the straight channel, and the most stable geometry we found is, as expected, the one where the smallest effective dimension of the fructose molecule intersects with the channel. Figure 4 illustrates the positions of the fructose adsorbed in the most stable configurations (a) at the channel intersection and (b) in the straight pore where the channel does not intersect with others. The PW91+D adsorption energy corresponding to the straight pore is −10.8 kcal/mol, with dispersion and PW91 energy contributions of −39.9 and 29.1 kcal/mol, respectively. The positive PW91 adsorption energy is a result of molecule and/or zeolite framework deformation, indicating that the molecule is too big to fit into the pore in a "comfortable" relaxed configuration. The fructose molecule adsorbed in this position is also away from the acidic site and thus lacks the stabilization from forming hydrogen bonds with the acidic site. However, the dispersion interaction in this adsorption configuration is rather large, so the adsorption is overall exothermic. Nevertheless, the adsorption energy of the molecule in the straight pore is much smaller than that in the channel intersections (the latter energy is −49.5 and −30.5 kcal/mol, respectively, with and without bonding with an acidic site at PW91 +D, indicating that the straight pore configuration is much less favorable than the intersection configuration, regardless of the contribution of acidic sites).

Thus, for a fructose molecule to migrate from one channel intersection to another, it has to travel through a series of high-energy positions in the straight channel, which makes the migration process energetically unfavorable and only likely at highly elevated temperature.

An alternative scenario of fructose diffusion in the ZSM-5 is that, at a high enough temperature, prior to diffusion, the molecule is converted to the acyclic form, which has a smaller kinetic diameter and diffuses more easily than the cyclic form. The adsorption energy of acyclic fructose in straight pore and channel intersections was calculated to be −24.7 and −47.3 kcal/mol, respectively. The 22.5 kcal/mol energy difference between the two adsorption positions of the acyclic fructose is much smaller than that of the cyclic form (38.7 kcal/mol), suggesting that the diffusion of the acyclic fructose should not be as unfavorable as the cyclic. Although fructose is more stable in the cyclic form (for example, in an HZSM-5 channel intersection, the cyclic fructose is 7.4 kcal/mol more stable than the acyclic form in their respective most stable, yet very similar, adsorption geometries), the cyclic fructose conversion to acyclic reaction barrier of <29 kcal/mol (periodic, DFT+D) is not prohibitively high. Thus, a scenario of fructose conversion from cyclic to acyclic and diffusion through ZSM-5 is viable. If the cyclic-to-acyclic conversion is rate-limiting, at a temperature of ∼438 K (the temperature that has been used for fructose dehydration in H-mordenites[4]), assuming a prefactor of 10^{13} s^{-1}, the calculated diffusion turnover rate is 0.03 s^{-1} per site. With zero-point correction (not calculated in this study), we also expect a small decrease in barriers due to the missing vibrational mode at the transition state. This will lead to an increase in turnover frequency, which makes the diffusion rate reasonable. Nevertheless, the mass transport of fructose in ZSM-5 is expected to be slow based on our calculated results.

4. CONCLUSIONS

From this computational study of fructose adsorption and protonation at an HZSM-5 acidic site, we reach the following important conclusions concerning modeling requirements.

Proper treatment of dispersion effects is absolutely necessary for calculations when large molecules are adsorbed in a zeolite framework. The inclusion of dispersion effects increases the magnitude of the adsorption energy by 31 kcal/mol and the protonation energy by 35 kcal/mol based on use of the Grimme correction added to the PW91 functional.

Finite-sized models, even as large as the 46T model, are not sufficient to accurately describe the energy profiles of reactions in zeolites. The adsorption energy calculated for the 46T model is 7.4 kcal/mol smaller than the periodic model value due to the slow convergence of long-range dispersion effects. However, the key geometric parameters calculated using the 46T model are very similar to those calculated with a periodic model.

On the basis of MP2/CBS calculations for the two reaction steps calculated in this work, the PW91+D reaction energies are reasonably accurate, as they agree to within 1.2 kcal/mol for adsorption and 3.9 kcal/mol for protonation.

On the basis of the periodic results, this study also provides important insight into the adsorption properties of fructose in a zeolite pore where there is a large molecule/surface contact area compared to a much smaller contact when interacting with a flat surface. As a result, although the contribution of dispersion interaction to normal binding energies is normally relatively small compared to chemical bonds, the accumulation of the interactions leads to a significant strengthening of the adsorbate bond. This type of stabilization effect is expected to be important for the adsorption of large molecules in other microporous materials, as well. The periodic results also indicate that proton transfer to fructose is favorable. Finally, our calculations predict that the diffusion of the cyclic form of fructose inside ZSM-5 might be limited, and conversion of the cyclic to acyclic at high temperature may be required for diffusion of fructose.

AUTHOR INFORMATION

Corresponding Author
*E-mail: curtiss@anl.gov.

ACKNOWLEDGMENT

This work was supported by the U.S. Department of Energy under Contract DE-AC0206CH11357. This material is based upon work supported as part of the Institute for Atom-efficient Chemical Transformations (IACT), an Energy Frontier Research Center funded by the U.S. Department of Energy, Office of Science, Office of Basic Energy Sciences, and by the German Research Foundation (DFG) within the Center of Excellence UNICAT, Berlin.

The research was performed using EMSL, a national scientific user facility sponsored by the U.S. Department of Energy's Office of Biological and Environmental Research and located at Pacific Northwest National Laboratory, and the ANL Center for Nanoscale Materials.

REFERENCES

(1) Chheda, J. N.; Huber, G. W.; Dumesic, J. A. *Angew. Chem., Int. Ed.* **2007**, *46*, 7164.
(2) Assary, R. S.; Redfern, P. C.; Greeley, J.; Curtiss, L. A. *J. Phys. Chem. B* **2011**, *115*, 4341.
(3) Mercadier, D.; Rigal, L.; Gaset, A.; Gorrichon, J. P. *J. Chem. Technol. Biotechnol.* **1981**, *31*, 489.
(4) Moreau, C.; Durand, R.; Razigade, S.; Duhamet, J.; Faugeras, P.; Rivalier, P.; Ros, P.; Avignon, G. *Appl. Catal., A* **1996**, *145*, 211.
(5) Kuster, B. F. M. *Starch/Staerke* **1990**, *42*, 314.
(6) Grin, S. A.; Tsimbalaev, S. R.; Gelfand, S. Y. *Kinet. Catal.* **1993**, *34*, 200.
(7) Elhajj, T.; Masroua, A.; Martin, J. C.; Descotes, G. *Bull. Soc. Chim. Fr.* **1987**, 855.
(8) Vandam, H. E.; Kieboom, A. P. G.; Vanbekkum, H. *Starch/Staerke* **1986**, *38*, 95.
(9) Rigal, L.; Gaset, A. *Biomass* **1985**, *8*, 267.
(10) Weisz, P. B.; Haag, W. O.; Rodewald, P. G. *Science* **1979**, *206*, 57.
(11) Carlson, T. R.; Vispute, T. R.; Huber, G. W. *ChemSusChem* **2008**, *1*, 397.
(12) Tuma, C.; Sauer, J. *Phys. Chem. Chem. Phys.* **2006**, *8*, 3955.
(13) Svelle, S.; Tuma, C.; Rozanska, X.; Kerber, T.; Sauer, J. *J. Am. Chem. Soc.* **2009**, *131*, 816.
(14) Hansen, N.; Krishna, R.; van Baten, J. M.; Bell, A. T.; Keil, F. J. *J. Phys. Chem. C* **2009**, *113*, 235.
(15) Grimme, S. *J. Comput. Chem.* **2006**, *27*, 1787.
(16) Kerber, T.; Sierka, M.; Sauer, J. *J. Comput. Chem.* **2008**, *29*, 2088.
(17) Hansen, N.; Kerber, T.; Sauer, J.; Bell, A. T.; Keil, F. J. *J. Am. Chem. Soc.* **2010**, *132*, 11525.
(18) Zygmunt, S. A.; Curtiss, L. A.; Zapol, P.; Iton, L. E. *J. Phys. Chem. B* **2000**, *104*, 1944.
(19) Lesthaeghe, D.; Van Speybroeck, V.; Marin, G. B.; Waroquier, M. *Chem. Phys. Lett.* **2006**, *417*, 309.

(20) Hemelsoet, K.; Nollet, A.; Vandichel, M.; Lesthaeghe, D.; Van Speybroeck, V.; Waroquier, M. *ChemCatChem* **2009**, *1*, 373.
(21) Kokotailo, G. T.; Lawton, S. L.; Olson, D. H.; Olson, D. H.; Meier, W. M. *Nature* **1978**, *272*, 437.
(22) Becke, A. D. *J. Chem. Phys.* **1993**, *98*, 5648.
(23) Perdew, J. P.; Burke, K.; Ernzerhof, M. *Phys. Rev. Lett.* **1996**, *77*, 3865.
(24) Perdew, J. P.; Wang, Y. *Phys. Rev. B* **1992**, *45*, 13244.
(25) Zhao, Y.; Schultz, N. E.; Truhlar, D. G. *J. Chem. Phys.* **2005**, *123*, 161103.
(26) Lesthaeghe, D.; De Sterck, B.; Van Speybroeck, V.; Marin, G. B.; Waroquier, M. *Angew. Chem., Int. Ed.* **2007**, *46*, 1311.
(27) Van Speybroeck, V.; Van der Mynsbrugge, J.; Vandichel, M.; Hemelsoet, K.; Lesthaeghe, D.; Ghysels, A.; Marin, G. B.; Waroquier, M. *J. Am. Chem. Soc.* **2011**, *133*, 888.
(28) Vankoningsveld, H.; Vanbekkum, H.; Jansen, J. C. *Acta Crystallogr., Sect. B: Struct. Sci.* **1987**, *43*, 127.
(29) Olson, D. H.; Kokotailo, G. T.; Lawton, S. L.; Meier, W. M. *J. Phys. Chem.* **1981**, *85*, 2238.
(30) Frisch, M. J.; Trucks, G. W.; Schlegel, H. B.; Scuseria, G. E.; Robb, M. A.; Cheeseman, J. R.; Scalmani, G.; Barone, V.; Mennucci, B.; Petersson, G. A.; Nakatsuji, H.; Caricato, M.; Li, X.; Hratchian, H. P.; Izmaylov, A. F.; Bloino, J.; Zheng, G.; Sonnenberg, J. L.; Hada, M.; Ehara, M.; Toyota, K.; Fukuda, R.; Hasegawa, J.; Ishida, M.; Nakajima, T.; Honda, Y.; Kitao, O.; Nakai, H.; Vreven, T.; Montgomery, Jr., J. A.; Peralta, J. E.; Ogliaro, F.; Bearpark, M.; Heyd, J. J.; Brothers, E.; Kudin, K. N.; Staroverov, V. N.; Kobayashi, R.; Normand, J.; Raghavachari, K.; Rendell, A.; Burant, J. C.; Iyengar, S. S.; Tomasi, J.; Cossi, M.; Rega, N.; Millam, N. J.; Klene, M.; Knox, J. E.; Cross, J. B.; Bakken, V.; Adamo, C.; Jaramillo, J.; Gomperts, R.; Stratmann, R. E.; Yazyev, O.; Austin, A. J.; Cammi, R.; Pomelli, C.; Ochterski, J. W.; Martin, R. L.; Morokuma, K.; Zakrzewski, V. G.; Voth, G. A.; Salvador, P.; Dannenberg, J. J.; Dapprich, S.; Daniels, A. D.; Farkas, Ö.; Foresman, J. B.; Ortiz, J. V.; Cioslowski, J.; Fox, D. J. *Gaussian 09*, revision A.1; Gaussian, Inc.: Wallingford, CT, 2009.
(31) (a) Kresse, G.; Hafner, J. *Phys. Rev. B* **1993**, *47*, 558. (b) Kresse, G.; Hafner, J. *Phys. Rev. B* **1994**, *49*, 14251. (c) Kresse, G.; Furthmuller, J. *Phys. Rev. B* **1996**, *54*, 11169. (d) Kresse, G.; Furthmuller, J. *Comput. Mater. Sci.* **1996**, *6*, 15.
(32) Valiev, M.; Bylaska, E. J.; Govind, N.; Kowalski, K.; Straatsma, T. P.; Van Dam, H. J. J.; Wang, D.; Nieplocha, J.; Apra, E.; Windus, T. L.; de Jong, W. *Comput. Phys. Commun.* **2010**, *181*, 1477.
(33) Curtiss, L. A.; Redfern, P. C.; Raghavachari, K.; Rassolov, V.; Pople, J. A. *J. Chem. Phys.* **1999**, *110*, 4703.
(34) Zygmunt, S. A.; Curtiss, L. A.; Iton, L. E. *J. Phys. Chem. B* **2001**, *105*, 3034.
(35) Limtrakul, J.; Chuichay, P.; Nokbin, S. *J. Mol. Struct.* **2001**, *560*, 169.
(36) Krossner, M.; Sauer, J. *J. Phys. Chem.* **1996**, *100*, 6199.
(37) Clark, L. A.; Sierka, M.; Sauer, J. *J. Am. Chem. Soc.* **2003**, *125*, 2136.
(38) Sauer, J. In *Handbook of Hydrogen Transfer*; Schowen, R. L., Klinman, J. P., Hynes, J. T., Limbach, H.-H., Eds.; Wiley-VCH: Weinheim, Germany, 2006; Vol. 2, p 685.
(39) Curtiss, L. A.; Redfern, P. C.; Raghavachari, K. *J. Chem. Phys.* **2007**, *126*, 084108.
(40) Tuma, C.; Kerber, T.; Sauer, J. *Angew. Chem., Int. Ed.* **2010**, *49*, 4678.
(41) Carton, A.; Benito, G. G.; Rey, J. A.; de la Fuente, M. *Bioresour. Technol.* **1998**, *66*, 75.